



The 28th Iranian Conference on
Optics and Photonics (ICOP 2022),
and the 14th Iranian Conference on
Photonics Engineering and
Technology (ICPET 2022).

Shahid Chamran
University of Ahvaz,
Khuzestan, Iran,
Feb. 1-3, 2022



بررسی نظری حسگر فیبر بلور فوتونی روباز مبتنی بر تشدید پلاسمون سطحی نانوسیم طلا

صغری قهرمانی، جمال بروستانی، و بهار مشگین قلم

دانشکده فیزیک دانشگاه تبریز

چکیده- یک حسگر فیبر بلور فوتونی روباز مبتنی بر تشدید پلاسمون سطحی با استفاده از نانوسیم طلا طراحی گردیده و با استفاده از روش تفاضل متناهی در حوزه زمان مطالعه شده است. در این ساختار به منظور حصول عملکرد بهتر حسگری، یک نانوایر طلا معرفی شده است. مشکلاتی که در پوشش دهی فیلم فلزی در سطح داخلی و خارجی فیبر بلور فوتونی ایجاد می شود با استفاده از نانوایر طلا از بین می رود. مشخصه حساسیت طول موجی و دامنه حسگر پیشنهادی ارائه شده است. این حسگر بیشترین حساسیت طول موجی بدست آمده $3090 \left[\frac{\text{nm}}{\text{RIU}} \right]$ و بیشترین حساسیت دامنه بدست آمده $314.4 \left[\frac{1}{\text{RIU}} \right]$ می باشد. انتظار می رود حسگر پیشنهادی قابلیت حسگری چند آنالیت را در کاربردهای زیستی و پزشکی داشته باشد.

کلید واژه- تشدید پلاسمون سطحی، حساسیت، حسگر اپتیکی، فیبر بلور فوتونی، نانوسیم.

Theoretical study of an Opening-up photonic crystal fiber sensor based on surface plasmon resonance employing gold nanowire

Soghra Ghahramani, Jamal Barvestani, and Bahar Meshginqalam

Faculty of Physics, University of Tabriz, Tabriz, Iran

Soghra.Ghahramani@tabrizu.ac.ir

Abstract- An opening-up photonic crystal fiber sensor based on surface plasmon resonance employing gold nanowire is designed and studied by the finite-difference time-domain method. To get the better sensing performance we introduce gold nanowire in this structure. Applying the gold nanowire can eliminate the problems of metal film coating in inner or outer surface of photonic crystal fiber. The performance of offered sensor has been described by wavelength and amplitude sensitivities. This sensor includes the maximum obtained wavelength and amplitude sensitivities of $3090 \left[\frac{\text{nm}}{\text{RIU}} \right]$ and $314.4 \left[\frac{1}{\text{RIU}} \right]$. It is expected that, the proposed sensor has capability of multi-analyte sensing in biological and medical applications.

Keywords: surface plasmon resonance, photonic crystal fiber, nanowire, sensitivity, optical sensor

1. Introduction

In recent years, surface plasmon resonance (SPR) sensor has attracted much attention due to their remarkable advantages such as high sensitivity, fast response, low-cost, capability of real-time sensing. Combination of photonic crystal fiber (PCF) and SPR sensor technologies widely used in a variety of research fields including drug discovery, food safety control, environment monitoring and development to medical diagnostics [1-3]. Two categories of SPR-based PCF sensors are internally metal-coated sensor and externally metal-coated sensor. In the first one, metal film are coated in the air holes with small size of micrometer while in the second one the PCF is coated with metal on the outer plane [4]. Xin yang et al. have proposed photonic crystal fiber-SPR liquid sensor based on elliptical detective channel. This elliptical sensing channel is introduced on the left side of the core which is coated with gold and the liquid is filled in it [5]. In externally metal coating sensor such as D-shaped PCF, the section of D-shaped needs polishing which is difficult process [6]. In 1400 Sakib et al. had suggested dual core D-shape PCF-based SPR sensor having wavelength sensitivity of 1000 [nm/RIU] and amplitude sensitivity of 100 [1/RIU] [7]. High-performance opening-up dual-core photonic crystal fiber sensor based on surface plasmon resonance had been proposed by Ghahramani et al. in which a large air hole introduced between two cores in opening-up section where was coated with gold and titanium dioxide layer. The given sensor showed maximum amplitude sensitivity of 1000 [1/RIU] [8]. In this work, we introduced plasmonic photonic crystal fiber sensor with gold nanowire as a plasmonic material. Complexities of metal deposition in inner or outer of SPR-PCF sensors can be removed by employing gold nanowire. Furthermore, this gold nanowire enhances the coupling between fundamental core and SPR modes which improves sensing performance. The wavelength and amplitude interrogation methods are used for investigation sensing performance of the proposed

sensor. The results reveal the maximum wavelength and amplitude sensitivities of 1000 [nm/RIU] and 100 [1/RIU]. In addition, this design has the ability to use as a multichannel sensor.

2. Design and numerical method

Figure 1, shows the schematic representation of the proposed sensor. Air holes with the pitch of Λ in this arrangement are in 3 different radii. The radii of smallest and largest air holes are denoted by r_s and r_b and the symbol r_a shows the radius of normal air holes. There is an opening-up section with the width of w in the offered sensor where analyte infiltrates in it. To improve the sensing performance, gold nanowire with the radius of r_{Au} is located in the center of this part.

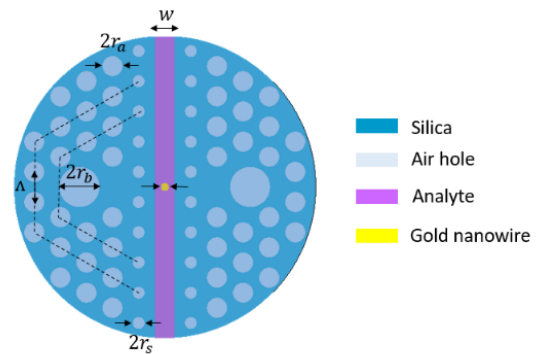


Fig. 1: Cross section view of the proposed sensor.

The optimized geometrical parameters of the offered sensor are set to be as follow: $r_s = 0.3 \mu\text{m}$, $r_b = 1 \mu\text{m}$, $r_a = 0.5 \mu\text{m}$, $w = 1 \mu\text{m}$, $\Lambda = 1.5 \mu\text{m}$. The refractive index of silica is obtained by the following Sellmeier equation [9]:

$$n_{\lambda}^2 = 1 + \frac{A_1 \lambda^2}{\lambda^2 - B_1} + \frac{A_2 \lambda^2}{(\lambda^2 - B_2)^2} + \frac{A_3 \lambda^2}{(\lambda^2 - B_3)^2}, \quad (1)$$

where $A_1 = 0.6961663$, $A_2 = 0.4079426$, $A_3 = 0.8974994$, $B_1 = 0.0684043$, $B_2 = 0.1162414$, $B_3 = 9.896111$ and λ implies operating wavelength in micrometer. The permittivity of gold nanowire is modeled from Johnson and Christy data. Simulation of the designed sensor is directed by using the finite-difference time-domain method (FDTD) based numerical software and a perfectly matched layer (PML) is applied as a scattering boundary condition.

Confinement loss is the key factor in calculation of sensor performance which is given as [9]:

$$\alpha_c \left(\frac{\text{dB}}{\text{cm}} \right) = 8.686 \times \frac{\pi}{\lambda(\mu\text{m})} \text{Im}(n_{\text{eff}}) \times 10^4, \quad (5)$$

where $\text{Im}(n_{\text{eff}})$ is the imaginary part of the effective refractive index.

3. Results and discussion

Figure 3 (a)- (c) illustrates the distribution of electric field of the fundamental mode, the surface plasmon mode and coupled fundamental core and SPR modes for the analyte refractive index (n_a) of 1.36. The effective refractive index of core and plasmonic mode becomes equal.

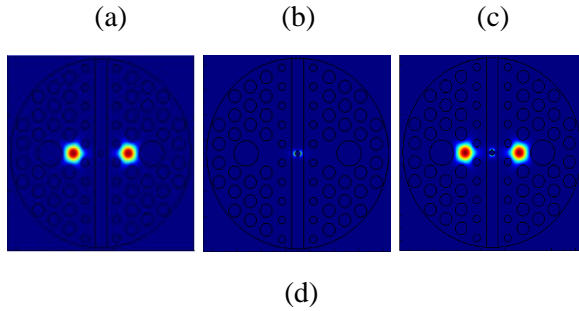


Fig. 3: Electric field distribution of (a) fundamental core mode, (b) SPR mode, (c) coupling of core and SPR modes and (d) the dispersion relation between the fundamental core mode and SPR mode at 0.93 μm with $r_{\text{Au}} = 0.2 \mu\text{m}$ and $n_a = 1.36$.

As you can see in panel 3 (a) electric field concentrates in core where at resonance wavelength, i.e. 0.93 μm, some part of electric field penetrate from core region towards gold nanowire and coupling between fundamental core and SPR

modes occur, as shown in panel (c). A sharp peak can be revealed as a result of penetration process which it is depicted in figure 3 (d). This condition is known as a phase matching condition where the real part of refractive index of SPR mode and core mode become equal. The small change in refractive index (RI) of analyte can be affected the SPR modes. Figure 3 shows the loss spectrum of core mode as a function of analyte RI variation, from 1.33 to 1.37.

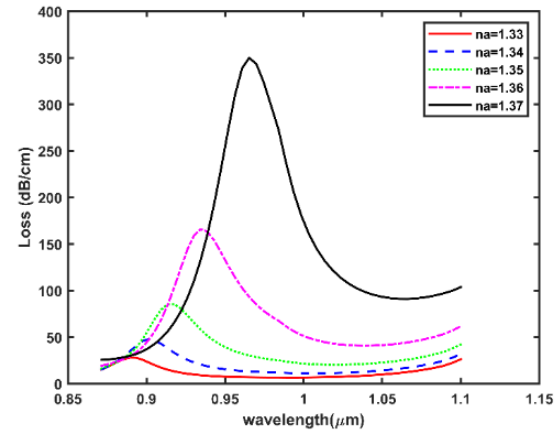


Fig. 3: Loss spectrum for different analyte RI.

It is obvious that, by increasing analyte RI the resonance wavelength red shifts and the confinement loss increases as well.

Wavelength sensitivity is one of important parameter for evaluation of sensor performance and it is defined as follows [10]:

$$S_w \left(\frac{\text{nm}}{\text{RIU}} \right) = \frac{\partial \lambda_{\text{peak}}}{\partial n_a}, \quad (6)$$

where ∂n_a denotes analyte RI variation. The proposed sensor shows the wavelength sensitivities of 118.0 [nm/RIU], 162.0 [nm/RIU], 168.0 [nm/RIU] and 309.0 [nm/RIU] when analyte refractive index varies from 1.33 to 1.37. The wavelength sensitivity is calculated by the given formula [10]:

$$S_A \left(\frac{1}{\text{RIU}} \right) = - \frac{1}{\alpha(\lambda, n_a)} \times \frac{\partial \alpha(\lambda, n_a)}{\partial n_a}, \quad (7)$$

where $\alpha(\lambda, n_a)$ is the confinement loss at different RI.

The amplitude sensitivity curves for different refractive index of analyte are demonstrated in Figure 4. We see that the maximum amplitude

sensitivity is $314.4 \left[\frac{1}{\text{RIU}} \right]$ which corresponds to variation of analyte RI from 1.33 to 1.37.

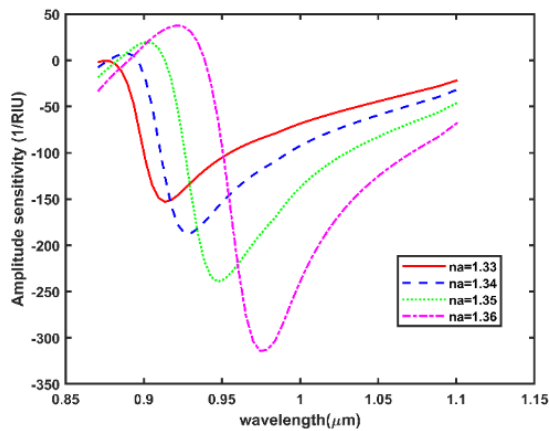


Fig. 5: Amplitude sensitivity of proposed sensor as a function of wavelength.

Amplitude sensitivities are computed as $103 \left[\frac{1}{\text{RIU}} \right]$, $187 \left[\frac{1}{\text{RIU}} \right]$, $239.4 \left[\frac{1}{\text{RIU}} \right]$ when analyte RI changes from 1.33 to 1.36, respectively.

5. Conclusion

In this paper, the performance of an opening-up photonic crystal fiber sensor based on surface plasmon resonance applying gold nanowire is investigated. Gold nanowire is located in the center of structure. Applying gold nanowire overcomes the problems of metal coating in PCF-SPR sensors and improved desirable coupling features. The finite-difference time-domain method based on numerical software is used for calculation of the proposed sensor performance. The maximum wavelength and amplitude sensitivities are calculated as $3090 \left[\frac{\text{nm}}{\text{RIU}} \right]$ and $314.4 \left[\frac{1}{\text{RIU}} \right]$. The proposed sensor has capability for using as multichannel sensor.

References

- [1] S. Chu, K. Nakkeeran, A. M. Abobaker, S. S. Aphale, S. Sivabalan, P. R. Babu, and K. Senthilnathan, "A Surface Plasmon Resonance Bio-Sensor Based on Dual Core D-Shaped Photonic Crystal Fibre Embedded With Silver Nanowires for Multisensing," *IEEE Sensors Journal*, vol. 21, no. 1, pp. 76-84, 2020.
- [2] T. Cheng, X. Li, S. Li, X. Yan, X. Zhang, and F. Wang, "Surface plasmon resonance temperature sensor based on a photonic crystal fiber filled with silver nanowires," *Applied Optics*, vol. 59, no. 17, pp. 5108-5113, 2020.
- [3] C. Liu, G. Fu, F. Wang, Z. Yi, C. Xu, L. Yang, Q. Liu, W. Liu, X. Li, and H. Mu, "Ex-centric core photonic crystal fiber sensor with gold nanowires based on surface plasmon resonance," *Optik*, vol. 196, pp. 163173, 2019.
- [4] M. R. Islam, A. Iftakher, K. R. Hasan, J. Nayan, S. B. Islam, M. M. I. Khan, J. A. Chowdhury, F. Mehjabin, M. Islam, and M. S. Islam, "Design and Analysis of a Biochemical Sensor Based on Surface Plasmon Resonance with Ultra-high Sensitivity," *Plasmonics*, vol. 16, no. 3, pp. 849-861, 2021.
- [5] X. Yan, Y. Wang, T. Cheng, and S. Li, "Photonic Crystal Fiber SPR Liquid Sensor Based on Elliptical Detecting Channel," *Micromachines*, vol. 12, no. 4, pp. 408, 2021.
- [6] M. N. Sakib, M. B. Hossain, K. F. Altabatabaie, I. M. Mehedi, M. T. Hasan, M. A. Hossain, and I. Amiri, "High performance dual core D-shape PCF-SPR sensor modeling employing gold coat," *Results in Physics*, vol. 15, pp. 102788, 2019.
- [7] S. Ghahramani, J. Bravestani, and B. Meshginqalam, "High Performance Opening Up Dual-core Photonic Crystal Fiber Sensor Based on Surface Plasmon Resonance," 2021.
- [8] H. Wang, W. Rao, J. Luo, and H. Fu, "A Dual-Channel Surface Plasmon Resonance Sensor Based on Dual-Polarized Photonic Crystal Fiber for Ultra-Wide Range and High Sensitivity of Refractive Index Detection," *IEEE Photonics Journal*, vol. 13, no. 1, pp. 1-11, 2021.
- [9] E. Haque, A. Al Noman, M. A. Hossain, N. H. Hai, Y. Namihira, and F. Ahmed, "Highly Sensitive D-Shaped Plasmonic Refractive Index Sensor for a Broad Range of Refractive Index Detection," *IEEE Photonics Journal*, vol. 13, no. 1, pp. 1-11, 2021.
- [10] V. Kaur, and S. Singh, "Design of D-Shaped PCF-SPR sensor with dual coating of ITO and ZnO conducting metal oxide," *Optik*, vol. 220, pp. 165135, 2020.